

Avoiding CFRP Delamination During Abrasive Water Jet Piercing: A New Piercing Method

Ioan Alexandru Popan (✉ ioan.popan@tcm.utcluj.ro)

Universitatea Tehnica din Cluj-Napoca <https://orcid.org/0000-0001-6003-8826>

Nicolae Bâlc

Alina Ioana Popan

Research Article

Keywords: abrasive water jet, piercing, delamination, composite materials, CFRP

Posted Date: August 2nd, 2021

DOI: <https://doi.org/10.21203/rs.3.rs-692901/v1>

License:  This work is licensed under a Creative Commons Attribution 4.0 International License.

[Read Full License](#)

Abstract

Carbon Fibre Reinforced Polymer (CFRP) is used in top industries like aerospace, automotive or medicine. Abrasive water jet (AWJ) technology has demonstrated its capacity in machining CFRP parts with a high dimensional accuracy due to its low mechanical loading, reduced machining temperature, high productivity, reduced tooling, and environmental friendliness. An important challenge when machining composite materials with AWJ is material delamination, determined by the high-speed water jet hitting the material during the piercing process. It is the ideal tool for cutting complex CFRP parts, in cases where the piercing point is outside of the workpiece. The challenge lies in machining features where material piercing is required, like holes, slots or internal contours.

This paper presents a method of piercing the composite materials with abrasive water jet, that can avoid delamination. The method requires adding the abrasive particles in the water jet at the very beginning of jet formation, thus obtaining a mixed abrasive water jet during the first impact with the composite workpiece. A new cutting system was designed and set up based on the proposed piercing method and was compared with a conventional AWJ cutting system. The insertion of the abrasive particles into the water jet was monitored by using acoustic emission (AE). An analysis of the influence of piercing parameters (water pressure, standoff distance, abrasive inlet angle and abrasive delay time) on the delamination was conducted. The process outcomes such as hole surface integrity, delamination, particles embedment, uncut fibers and dimensional characteristics, were evaluated. The results show that the method is promising in reducing delamination.

1. Introduction

During the last decades, Carbon Fibre Reinforced Polymer (CFRP) was frequently used in areas such as aerospace, automotive, civil engineering, ships and medicine [1–6] because of their distinctive properties: high strength and stiffness, reduced weight, resistance to corrosion [1–6] and design flexibility [2]. For example, the Boeing 787 Dreamliner has over 50% of components (fuselage, wings, tail, doors and interior) made from composite materials which significantly improved its performance [1, 3–5].

AWJ technology has demonstrated its capacity in machining of composite materials, like CFRP [2, 5–10]. It is suitable for many processing applications like cutting [5], drilling [6], milling [8] and turning [9] because of its low mechanical loading, reduced machining temperature, high productivity, reduced tooling and environmental friendliness [2, 5–11]. AWJ cutting is the ideal tool for trimming complex parts made from CFRP. For example, in case of the Airbus 350 and Boeing 787 the composite stringers used for the T-Beam and I-Beam stiffeners are trimmed using AWJ [5, 12]. General Electric are using AWJ cutting for trimming composite fan blades on the GEnx engine [5]. By precisely controlling the depth of cut, AWJ is capable of milling pockets in composite materials [8]. Weiyi Lia et al. [9] demonstrated that the AWJ is a solution for turning CFRP cylindrical parts. AWJ machining is an efficient alternative for machining holes in CFRP materials [2, 13–18].

The material deterioration due to the shock created by the high-velocity waterjet hitting the material is an important problem in composites machining with AWJ [2, 6, 13–18]. This phenomenon takes place at the beginning of the piercing process. This is avoided in case of trimming or external contour cutting, by selecting a starting point outside of the workpiece. The challenge is to machine different features like holes, slots or internal contours, where a piercing of the composite material is required [19].

The AWJ process consists of a water jet (WJ) at high pressure mixed with abrasive particles (Fig. 1a), in order to process a variety of materials. Water is pumped at high pressure through a small orifice to create a high speed WJ, that accelerates the abrasive particles at a high speed, generating kinetic energy. The WJ stream reaches the mixing chamber where abrasive particles are mixed in. The abrasive particles reach the mixing chamber through an inlet tube and are pulled in gravitationally and by the suction generated by the WJ. The resulting AWJ is oriented towards the material through a focussing tube [7, 10, 11].

a. The AWJ working principle; b. The mechanism of composite material delamination.

Piercing composite materials with AWJ can create several defects like delamination, cracking, fiber pull-out or abrasive embedment. The most common defect while machining composite material with AWJ is delamination of the layers [13–18, 20]. Delamination can appear in all sections of the material (Fig. 1b): the upper (peel-up delamination), middle or bottom sections (push-out delamination) [21]. Several methods are used to evaluate the level of delamination: the maximum crack length [14], the delamination planar area [2], the delamination factor [21] or the delamination extent [13, 18]. Delamination often occurs when piercing composite material is required, like when machining features such as holes, slots or pockets [19].

Shanmugam et al. [14] noted that delamination takes place in two stages: the initial generation of cracks and the propagation of cracks. The initial cracks occur due to the shock wave caused by the high-velocity WJ impacting the material. This happens at the beginning of the piercing process before any abrasive particles are introduced. The propagation of the cracks is a result of penetration of the water at a high pressure, into the initial cracks, causing a water-wedge action. AWJ characteristics like the kinetic energy rate, jet velocity and jet-workpiece interaction time, are directly correlated with the delamination mechanism [14, 17].

AWJ piercing parameters (water pressure, standoff distance, abrasive mass flow, abrasive inlet angle, delay time, material thickness, orifice diameter, focusing tube diameter) can influence CFRP delamination [2, 13–18]. Shanmugam et al [14] researched the influence of AWJ piercing parameters on CFRP delamination. They proposed an energy conservation model to predict the extent of delamination. Experimental results indicate that delamination could be reduced by decreasing the jet diameter and water pressure. Phapale et al. [13] observed that, by increasing water pressure, the kinetic energy of the AWJ raises, resulting a higher delamination. A low standoff distance affects the AWJ divergence and can reduce the delamination. Experimental studies also showed that abrasive mass flow has less of an effect

Loading [MathJax]/jax/output/CommonHTML/fonts/TeX/fontdata.js ce. It was observed that by increasing the

abrasives mass flow, delamination slightly decreases [2, 13, 14]. Garam et al. [2] recommends using low pressure (under 148 MPa) for piercing, to decrease the delamination area, and switching to a higher pressure for the cutting process itself. Delamination could be considerably reduced by using an optimum set of process parameters, but it cannot be fully avoided [22].

Homogeneity and stability of the AWJ flow also affect delamination during piercing [2, 14]. In the early stage of the AWJ formation, abrasive particles can reach the mixing chamber before the WJ [14] and can clog the mixing chamber. This can be prevented by delaying the abrasive flow [14] with 0 to 2 seconds [2]. Garam et al. [2] demonstrated that delamination could be reduced or even eliminated if the mixture of abrasive particles and WJ is stabilized at the beginning of the piercing process.

There are several types of cutting head designs with different values of abrasive inlet angle (Ψ) which has a direct influence in the AWJ formation process. This angle can have different values depending on the equipment manufacturer: 90° for KMT and Omax, 60° for Flow, and 40° for AccuStream. Nevertheless, there are a few studies regarding the effect of the Ψ on AWJ formation and the process quality characteristics.

The three main types of piercing methods used in AWJ machining are: stationary piercing, dynamic piercing and drilling [2, 23–26]. Stationary or static piercing is the most basic piercing method and can be used for a large variety of materials. The nozzle remains fixed in the hole centre while the AWJ pierces the material [2, 25]. This piercing method takes a long time, especially in thicker materials but it has the advantage of small hole diameter and that it is easy to program [25]. Dynamic piercing methods involve the AWJ moving relative to the hole centre, during the piercing process. This piercing method avoids the interference of the incoming jet with the reflected one during piercing. The jet movement is linear or circular. In linear piercing, the water jet moves in a straight line (1–3 mm) along the cutting path while during circular piercing, the AWJ moves in a 2–3 mm diameter circle around the hole centre [2, 23–26]. Dynamic piercing is the main type of piercing used in manufacturing because it is much faster than stationary piercing. Thongkaew et al. [6] suggested that pre-drilling a starter hole could eliminate the composites material delamination. Some AWJ machines can be accessorised with an extra spindle, used for drilling [23] but it can result in a higher machining time and costs.

2. Purpose Of The Research

The present paper proposes and demonstrates a new method of AWJ piercing of advanced composite materials, that reduces or eliminates delamination.

To this purpose, a cutting system was designed based on the proposed method and it was compared with a conventional AWJ cutting system within an experimental study.

It was followed by an analysis of the influence piercing parameters (water pressure, standoff distance, abrasive inlet angle and abrasive delay time) on the delamination using the Response Surface

Finally, an evaluation of the surface integrity of the holes was made to study delamination, particles embedment, uncut fibers and dimensional characteristics.

3. The Proposed Method For Abrasive Water Jet Piercing

The problem addressed by the new method is the lack of abrasive particles in the WJ as it hits the material in the beginning of the piercing process. The concept consists of adding the abrasive particles into the mixing chamber at the very beginning of the jet formation. Obtaining a homogeneous AWJ on the early stages of the piercing process can reduce or avoid the composite materials delamination.

In conventional cutting applications, the abrasive particles are introduced into the mixing chamber after the WJ start, with a delay, that is introduced through the cutting system design or intentionally, to avoid the clogging of the mixing chamber [2]. The WJ hits the composite material without any abrasive material and the resulting shock creates delamination [14].

A cutting system must be designed to add the abrasive particles into mixing chamber through gravitational flow. Figure 2 shows the proposed cutting system for composite materials piercing.

Opposite to the conventional system, in the proposed design, the abrasive particles are introduced in the mixing chamber through an abrasive inlet tube oriented at an angle causing the abrasive particles to be added to the jet from the beginning. After jet stabilization the suction generated by the WJ and gravitational flow provide a constant mass flow rate of abrasive particles.

The main component of the system is the cutting head. It is required to use a cutting head with an abrasive inlet tube orientated at $\Psi = 40-60$ deg. The abrasive delivery system is another key component. An electronic system must be installed on the upper part of the cutting system and it must accurately control the abrasive flow rate and the abrasive start moment. Cutting head and abrasive delivery system are connected in a vertical line through a tube. The internal diameter of the abrasive delivery system must be at least 3 mm to be able to provide the abrasive particles flow and to eliminate the air from the mixing chamber.

An efficient AWJ piercing process of composite materials depends on:

1. The cutting system design. The method requires to use a cutting system which can introduce the abrasive particles into the mixing chamber through a flow, based on the gravitational force.
2. The synchronization of the start of the WJ with the start of the flow of abrasive. If the WJ starts before the abrasive, it hits the material without abrasive, causing delamination. If the abrasive flow starts before the WJ, it can clog up the mixing chamber.
3. The selection of suitable piercing process parameters (P , m_a , SOD) is also paramount.

4. Experimental Setup

To validate the proposed AWJ piercing method, a set of experimental trials have been conducted. The research uses the Response Surface Methodology (RSM) for the analysis, as it is recognized as a proper solution for studying AWJ processes [13, 17, 20, 27]. Central Composite Design (CCD) is a method that was selected as the experimental design which is suitable in RSM because of its good statistical properties. The water pressure (P) and the stand-off distance (SOD) are independent variables ($k = 2$) while the delamination extent (D_{ext}) is the output variable. Thirteen experimental runs (with three repetitions) were conducted and the results are presented in Table 1. Each factor is varied over 5 levels: $2^k = 4$ axial points, $2^k = 4$ factorial points and the centre points $2k = 6$.

Table 1
Process parameters used in the experimental trials.

Parameters	Values
Water Pressure, MPa (P)	100 136.61 225 313.39 350
Stand-off distance, mm (SOD)	1 1.73 3.5 5.27 6
Abrasive inlet angle, deg. (Ψ)	40 90
Abrasive start delay time, s	0.2
Abrasive mass flow, kg/min (m_a)	0.45
Abrasive type	Australian Garnet
Abrasive size, mesh	80
Focusing tube angle, deg.	90

The composite fiber reinforced polymer (CFRP) was used in this experimental study. The workpiece, with a 3 mm thickness, was manufactured through a heat pressing process. The prepreg was made from a 3k-fabric style 452 in twill weave 2/2 and a quantity of 364 g/m² epoxy resin. The specimens were trimmed by AWJC at 100 x 70 mm.

The cutting was performed with a Omax 2626 machine (Fig. 3a) equipped with an ultra-high pressure (UHP) cutting system. The water pressure (P) can be varied between 100 and 350 MPa, using a direct UHP pump. The machine is equipped with an Alffi abrasive delivery system which can automatically adjust the abrasive mass flow rate (m_a) ranging from 0.05 to 0.6 kg/min. It is controlled with an OMAX CNC control system, which can move the cutting head in 3 axis simultaneously. A clamping system (Fig. 3b) was manufactured to fix the specimens on the worktable.

Table 2 presents the specifications of the two cutting systems designed for these experimental trials. The systems can be seen in Fig. 4.

Table 2
The experimental cutting systems specifications.

System	Conventional (CS90)	Proposed (CS40)
Cutting head	Dialine AccuStream	Carat 3.0 Gardella
Abrasive inlet angle	$\Psi = 90$ deg.	$\Psi = 40$ deg.
Orifice	Diamond, $d_o=0.35$ mm	Diamond, $d_o=0.35$ mm
Focusing tube	Rotec 500 ($d_f=0.76$ mm / $l_f=101$ mm)	Cerazitit WJNS ($d_f=0.76$ mm / $l_f=101,6$ mm)

The conventional cutting system (CS90), recommended by Omax, has the abrasive delivery system fixed on the right side of the cutting head, as it is shown in Fig. 4a. In the case of the proposed cutting system (CS40), the abrasive delivery system was fixed above the cutting head, aligned with it (Fig. 4b).

The abrasive flow and WJ start times were synchronized through an experimental study. Omax software (Omax Make) offers the possibility to set the abrasive flow start in relation to the pump start. The abrasive start delay time was varied between 0 and 2 s, with 0.1 increments while the rest of the cutting parameters were held constant ($P = 100$ MPa, $SOD = 1$ mm, $m_a = 0.45$ kg/min). There is no need for complex monitoring techniques or equipment to detect the clogging of the mixing chamber, as the WJ flows through the abrasive inlet tube instead of the focusing tube when this happens.

- In case of the conventional cutting system (CS90) the mixing chamber clogging phenomenon was not detected. The abrasive delivery system was fixed on the right side of the cutting head (Fig. 4a) and the abrasive particles were flowing downwards in the abrasive tube and stopping close to the cutting head. The abrasive grains are added in the cutting head through the suction generated by the water jet.
- For the new proposed cutting system (CS40) the mixing chamber clogging phenomenon was avoided by selecting 0.2 s as the abrasive start delay time. By fixing the abrasive delivery system vertically above the cutting head and an abrasive inlet tube oriented at 40 deg. (Fig. 4b), the abrasive particles were flowing directly to the mixing chamber at the same time with the water jet.

After determining the optimal synchronization time for the abrasive flow and water jet, the 13 experimental trials were carried out. The delamination extent was determined by cross-sectioning each specimen (Fig. 5.a) and observing it with two optical microscopes Optika B-1000 and Guhring PG 2000 (Table 3).

The delamination extent D_{ext} (Fig. 5b) was calculated with the formula [13, 18]:

$$D_{ext} = (D_{max} - D_{nom})$$

where:

D_{\max} is the maximum diameter of delamination area,

D_{nom} is the nominal hole diameter.

Table 3. The experimental results

Run	Water pressure, MPa (P)	Stand-off distance, mm (SOD)	Delamination extent, mm (D_{ext})	
			CS40	CS90
1	136.61	5.27	1.1	8.3
2	313.39	1.73	28.5	30.9
3	225.00	3.50	12.2	18.5
4	136.61	1.73	0.0	6.8
5	225.00	3.50	13.5	20.1
6	225.00	3.50	12.8	22.3
7	225.00	1.00	10.2	19.4
8	350.00	3.50	34.6	48.2
9	225.00	3.50	14.9	25.5
10	225.00	3.50	12.2	22.3
11	313.39	5.27	29.5	29.7
12	100.00	3.50	0.0	5.2
13	225.00	6.00	18.1	26

5. Results And Discussions

The specimens were analysed from the perspective of the machined surface morphology. The piercing process was monitored using Acoustic Emissions (AE) and the resulting signals were analysed. Finally, the effects of the piercing parameters on material delamination were determined.

5.1 Morphology of the machined surfaces

The machined surfaces were analysed under a microscope to understand the CFRP behaviour during the piercing process (cracks, delamination, particle embedment, uncut fibers or plastic deformation of the matrix). The main machined zones were analysed: initial damage zone (IDZ), smooth cutting zone (SCZ)

Delamination was observed in all 13 specimens pierced with the conventional system (CS90) while this phenomenon was observed for only 11 (out of 13) trials for the proposed system (CS40). A typical delamination of CFRP during the piercing process looks like in Fig. 6, that was obtained with the conventional system (CS90) during trial run no. 8 ($P = 350$ MPa, $Sod = 3.5$ mm, $m_a = 0.45$ kg/min). The delamination appears in all zones.

In Fig. 6b is shown the delamination of the bottom fibre layer (RCZ) and some pulled out or uncut fibres. It was observed also on some specimens in IDZ and it appeared in the experimental trials where a high pressure of over 300 MPa was used. In Fig. 6c the top fibre layer delamination is shown. It is also noticed that, in a few cases, abrasive particles are embedded inside the delamination cracks.

In 70% of the experimental trials the delamination appears in SCZ and RCZ.

No delamination was present in two experimental runs on the CS40, namely: run number 4 ($P = 136.61$ MPa, $SOD = 1.73$ mm) and run number 12 ($P = 100$ MPa, $SOD = 3.5$ mm). Both experimental trials were made using a low water pressure (under 137 MPa). This observation indicates that composite material delamination is correlated with the process parameters. The hole obtained in experimental run number 12 (Fig. 7) shows a good quality, smooth surface ($Ra = 3.1$ μm). The hole diameter varies from $\varnothing 1.37$ mm at the top of the hole to $\varnothing 1.21$ mm at the bottom. On the top part of the pierced hole (IDZ) a fillet was created with a radius of 0.21 mm (Fig. 7a, c) while the bottom edge (RCZ) remained sharp and the bottom fibre layer is not delaminated (Fig. 7b).

5.2 The piercing process analysis via acoustical emissions AE

To validate this concept an experimental study was made. Acoustic Emission (AE) was used to detect the moment when the abrasive particles are added in the WJ. The new proposed cutting system CS40 was compared with a conventional cutting system CS90, evaluating the abrasive particles adding time in the WJ.

This non-destructive testing is based on monitoring the transient elastic waves inside the material called acoustic emissions [27]. This technique is a proper solution for monitoring AWJ technologies [28, 29] because the AE signals can offer information about the changes of AWJ characteristics, cutting system malfunction, crack formation/propagation on the workpiece or material removal [27–29].

The AE signal acquisition system employed was composed of a data acquisition (DAQ) board, preamplifiers and the AE sensors (Fig. 8). The DAQ board, a PCI-6110 from National Instruments, can acquire data through four channels, at a sample rate of up to 5M samples/s. The AE sensors were connected to the DAQ board through a NI 2110 connection box. The data acquisition program, developed in NI LabView 2015 and NI DIAdem 2015, was used for signal analysis. The AE-sensor Vallen VS900-M that was used is a passive piezoelectric sensor with a response frequency (f_{Peak}) between 100 and 900

kHz. The Physical Acoustic preamplifier 2/4/6 was selected to amplify the signal and a gain of 40 dB was selected to acquire a clear AE signal.

Three cases were monitored using AE:

1. Piercing without abrasive on the CS40 ($P = 100$ MPa, $SOD = 0.5$ mm, $m_a = 0$ kg/min, $\Psi = 40^\circ$)
2. Piercing with abrasive on the CS90 ($P = 100$ MPa, $SOD = 0.5$ mm, $m_a = 0.45$ kg/min, $\Psi = 90^\circ$)
3. Piercing with abrasive on the CS40 ($P = 100$ MPa, $SOD = 0.5$ mm, $m_a = 0.45$ kg/min, $\Psi = 40^\circ$)

Each experimental trial was repeated 5 times to ensure consistency and the same 3 mm thickness CFRP workpiece material like in the main experiment was used.

The AE signal acquired from the cutting head shows the moment when the abrasive particles get added to the WJ (Fig. 9). The peak amplitude and signal duration were evaluated. In all cases the WJ was started at about 1.2 s from process start.

In the first case (piercing without abrasive on the CS40), the average height of the peak amplitude was around 0.6 V for the whole process (Fig. 9a). The resulting delamination was high ($D_{ext} > 40$ mm) and the specimens were almost separated in two pieces.

In the second case (piercing with abrasive on the CS90), the abrasive and water are mixed 0.4 s after the start of the water jet (Fig. 9b). The medium height of the peak amplitude of the signal rises from 0.7 V (water jet only) to 5.6 V (water jet with abrasive). The material did show delamination, but to a smaller extent ($D_{ext} = 7$ mm).

In the last case (piercing with abrasive on the CS40), the abrasive particles were added into the water jet almost immediately after its start (0.039s), as can be seen in Fig. 9c. No delamination was present in this case.

In the conventional system, the abrasive particles are pulled into the water jet through suction. This creates almost a 0.5 s delay, leading to delamination. By using the proposed system, the particles are gravitationally pulled into the WJ and they are added almost instantly (0.039 s). By decreasing the adding time of the abrasive particles in WJ the material delamination could be reduced or avoided.

5.3 Effects of piercing parameters on material delamination

An analysis of the piercing process parameters (water pressure, standoff distance, abrasive inlet angle or abrasive delay time) was also made as they affect the composite material delamination.

Effects of water pressure and standoff distance on material delamination

Based on RSM, the effects of the independent variables (P and SOD) on the output variable (D_{ext}) were analysed. This method was involved in building the response surface model for predicting the

delamination extent. The experimental data for the proposed cutting system CS40 was analysed with the Design Expert 2019 software.

Multiple models were fit (linear, two factor interaction, quadratic and cubic) and the lack of fit test was used to determine how well each model fits the data (Table 4). The $\alpha = 0.05$ level of significance was chosen for the test. Some significant models were found ($p < 0.05$) but the quadratic model fit the data best ($R^2_{adj} = 0.977$, $p = 0.012$).

Table 4
The fitted model analysis

Lack of Fit Tests for the delamination extent (D_{ext})					
Source	Sum of Squares	df	Mean Square	F Value	p-value
Linear	57.98	6	9.66	25.98	0.0036
2FI	56.54	5	11.31	30.40	0.0028
Quadratic	16.79	3	5.60	15.05	0.0121
Cubic	0.54	1	0.54	1.45	0.2944
Pure Error	1.49	4	0.37		
Model Summary Statistics for the delamination extent (D_{ext})					
Source	Std. Dev.	R-Squared	Adjusted R-Squared	Predicted R-Squared	PRESS
Linear	2.44	0.9568	0.9481	0.9158	115.89
2FI	2.54	0.9578	0.9438	0.8820	162.43
Quadratic	1.62	0.9867	0.9772	0.9115	121.75
Cubic	0.64	0.9985	0.9965	0.9732	36.94

Table 5
The ANOVA table for the delamination extent (D_{ext})

Source	β	Sum of Squares	df	Mean Square	F Value	p-value
Model		1357.91	5	271.58	103.98	< 0.0001
AWJ Pressure (P)	12.63	1276.36	1	1276.36	488.69	< 0.0001
Standoff Distance (SOD)	2.25	40.36	1	40.36	15.45	0.0057
P*SOD	0.6	1.44	1	1.44	0.55	0.4819
P ²	2.39	39.74	1	39.74	15.21	0.0059
SOD ²	0.27	0.51	1	0.51	0.19	0.6728
Residual		18.28	7	2.61		
Lack of Fit		16.79	3	5.60	15.05	0.0121
Pure Error		1.49	4	0.37	103.98	< 0.0001
Cor Total		1376.19	12			

For the quadratic model, both the AWJ pressure and the standoff distance have significant influences (Table 5) while the interaction term is not significant (A*B). The resulting equation for the regression model is:

$$D_{ext} = 12.63 * P + 2.25 * SOD - 0.6 * P * SOD + 2.39 * P^2 + 0.27 * SOD^2 + 12.68$$

2

where:

D_{ext} - delamination extent (mm),

P - water pressure (MPa),

SOD - stand-off distance (mm).

The model was validated experimentally by conducting twelve trials. The maximum difference between the experimental values and the calculated values was 11 %.

The delamination extent is mainly influenced by the AWJ pressure (P) as seen in Fig. 10a. An increase in pressure from 136 to 313 MPa, increases the deamination extent (D_{ext}) from 3 to 27 mm. The stand-off distance (SOD) has a smaller influence on the delamination extent (Fig. 10b). Increasing the SOD from 1.73 to 5.27 mm results in an increase in D_{ext} from 9.3 to 15.4 mm. By reducing both AWJ pressure and

the standoff distance, the delamination extent can be reduced or even eliminated (Fig. 10c). The study outcome is comparable to other studies on AWJ piercing.

Effects of abrasive inlet angle and delay time on material delamination

In these experimental studies the abrasive inlet angle Ψ (Fig. 2) has a significant influence on the abrasive particles flowing into the WJ. Two cutting systems with 40 deg. and 90 deg. abrasive inlet angle were analysed.

During the trials made by using the cutting system CS90 (Fig. 4a) with $\Psi = 90$ deg., the abrasive particles were flowing downwards in the abrasive tube and stopping close to the cutting head. The abrasive was added in the cutting head through the suction generated by the waterjet. Due to this reason, the mixing chamber clogging phenomenon did not appear. This results in the water jet hitting the part without any abrasive, causing delamination in the material. In the experimental trials with this cutting head, the delamination was not fully avoided.

In the experimental trials done with the cutting system CS40 (Fig. 4b), with $\Psi = 40$ deg., the abrasive particles are flowing gravitationally into the mixing chamber in a very short interval. If the abrasive arrives in the mixing chamber before the water jet, it can clog up the mixing chamber. This problem is solved by introducing abrasive with a delay time. The start of the WJ was synchronized with the start of the flow of abrasive particles that was added into the WJ in the early stages of the jet formation. By contrast with CS90, delamination did not appear while using the CS40 system when using low AWJ pressures.

Using the optimal process parameters and a low value of the abrasive inlet angle the material delamination was avoided.

Conclusions

The composite material delamination mechanism takes place during the shockwave generated by the high-speed water jet impacting the material.

This paper presents a new method of piercing composite materials (CFRP) with abrasive water jet that reduces or avoids delamination.

The new method of adding the abrasive particles into the mixing chamber at the very beginning of the jet formation, showed better results, using an abrasive inlet angle of 40°, instead of 90°.

The moment when the abrasive particles should be added was identified by using Acoustic Emission. By reducing the time when the abrasive particles were added to the water jet from approximately 0.4 s to 0.04 s, delamination was reduced and for some parts even avoided.

The most significant parameter for the composite delamination is the water pressure. A low water pressure and low standoff distance are recommended, to minimize the delamination. The experimental

results showed that, during the composite material piercing process it is recommended to use a water pressure lower than 136 MPa and a standoff distance lower than 3.5 mm.

Optimizing the process parameters is recommended to avoid delamination, but the homogeneity of the abrasive water jet on the early stages of the piercing process is also important.

The delamination was observed in a large number of specimens through the analysis of the holes surface morphology. In 70% of the experimental trials the delamination appears on the middle section and push-out delamination on the bottom. In a few cases, uncut fibbers and abrasive particles embedded inside the cracks were observed. In the experimental trials where the delamination was avoided, a well-defined hole and good quality surface was obtained.

The proposed method is simple, quick setup and no special equipment is required. It can be implemented on any kind of AWJ industrial machine tool, used for manufacturing composite parts.

Abbreviations

AE - acoustic emission

AWJ - abrasive water jet

CCD - central composite design

CFRP - carbon fiber reinforced polymer/plastic

DoE - design of experiments

IDZ - initial damage zone

UHP - ultra high-pressure pump

RSM - Response Surface Methodology

RCZ - rough cutting zone

SCZ - smooth cutting zone

Declarations

Acknowledgement

This research was supported by HORIZON 2020 – DiCoMI Project, “Directional Composites through Manufacturing Innovation”, GA Nr. 778068.

Nomenclature

Loading [MathJax]/jax/output/CommonHTML/fonts/TeX/fontdata.js

D_{ext} - delamination extent [mm]

D_{max} - the maximum diameter of delamination [mm]

D_{nom} - the nominal hole diameter [mm]

d_o - water orifice diameter [mm]

d_f - focusing tube diameter [mm]

l_f - focusing tube length [mm]

m_a - abrasives mass flow [kg/min]

P - water pressure [MPa]

R_a - surface roughness [μm]

r_k - the top edge radius [mm]

t - material thickness [mm]

SOD - stand-off distance [mm]

Ψ - abrasive inlet angle [degree]

Funding

This research was supported by HORIZON 2020 – DiCoMI Project, “Directional Composites through Manufacturing Innovation”, GA Nr. 778068.

Conflicts of interest/Competing interests - Not applicable.

Availability of data and material - Not applicable.

Code availability - Not applicable.

Ethics approval - Not applicable.

Consent to participate - Not applicable.

Consent for publication

The authors agreed with the submission of the manuscript to the journal.

Authors' contributions

Loading [MathJax]/jax/output/CommonHTML/fonts/TeX/fontdata.js

All authors contributed to design the proposed method. I.A.P and A.I.P. carried out the experiments. A.I.P. performed the measurements and optical analysis. All authors analysed the experimental results and wrote of the manuscript.

References

1. Aamir M, Tolouei-Rad M, Giasin K, Nosrati A (2019) Recent advances in drilling of carbon fiber-reinforced polymers for aerospace applications: a review. *Int J Adv Manuf Technol* 105:2289–2308 . <https://doi.org/10.1007/s00170-019-04348-z>
2. Kim G, Denos BR, Sterkenburg R (2020) Influence of different piercing methods of abrasive waterjet on delamination of fiber reinforced composite laminate. *Composite Structures* 240:112065 . <https://doi.org/10.1016/j.compstruct.2020.112065>
3. Jia Z, Chen C, Wang F, Zhang C, Wang Q (2020) Analytical model for delamination of CFRP during drilling of CFRP/metal stacks. *Int J Adv Manuf Technol* 106:5099–5109 . <https://doi.org/10.1007/s00170-020-05029-y>
4. Xu J, Zhou L, Chen M, Ren F (2019) Experimental study on mechanical drilling of carbon/epoxy composite-Ti6Al4V stacks. *Materials and Manufacturing Processes* 34:715–725 . <https://doi.org/10.1080/10426914.2019.1594275>
5. Hashish M (2013) Trimming of CFRP aircraft components. WJTA-IMCA Conference and Expo September 9-11
6. Thongkaew K, Wang J, Li W (2019) An investigation of the hole machining processes on woven carbon-fiber reinforced polymers (CFRPs) using abrasive waterjets. *Machining Science and Technology* 23:19–38 . <https://doi.org/10.1080/10910344.2018.1449217>
7. Liu X, Liang Z, Wen G, Yuan X (2019) Waterjet machining and research developments: a review. *Int J Adv Manuf Technol* 102:1257–1335 . <https://doi.org/10.1007/s00170-018-3094-3>
8. Srinivasu DS, Axinte DA (2014) Mask-Less Pocket Milling of Composites by Abrasive Waterjets: An Experimental Investigation. *Journal of Manufacturing Science and Engineering* 136: . <https://doi.org/10.1115/1.4027181>
9. Li W, Zhu H, Wang J, Huang C (2016) Radial-mode abrasive waterjet turning of short carbon-fiber-reinforced plastics. *Machining Science and Technology* 20:231–248 . <https://doi.org/10.1080/10910344.2016.1165836>
10. Natarajan Y, Murugesan PK, Mohan M, Liyakath Ali Khan SA (2020) Abrasive Water Jet Machining process: A state of art of review. *Journal of Manufacturing Processes* 49:271–322 . <https://doi.org/10.1016/j.jmapro.2019.11.030>

11. Alsoufi MS (2017) State-of-the-Art in Abrasive Water Jet Cutting Technology and the Promise for Micro- and Nano-Machining. *International Journal of Mechanical Engineering and Applications* 5:1 . <https://doi.org/10.11648/j.ijmea.20170501.11>
12. Bañon F, Sambruno A, Batista M, Simonet B, Salguero J (2020) Study of the surface quality of carbon fiber–reinforced thermoplastic matrix composite (CFRTP) machined by abrasive water jet (AWJM). *Int J Adv Manuf Technol* 107:3299–3313 . <https://doi.org/10.1007/s00170-020-05215-y>
13. Phapale K, Singh R, Patil S, Singh RKP (2016) Delamination Characterization and Comparative Assessment of Delamination Control Techniques in Abrasive Water Jet Drilling of CFRP. *Procedia Manufacturing* 5:521–535 . <https://doi.org/10.1016/j.promfg.2016.08.043>
14. Shanmugam DK, Nguyen T, Wang J (2008) A study of delamination on graphite/epoxy composites in abrasive waterjet machining. *Composites Part A: Applied Science and Manufacturing* 39:923–929 . <https://doi.org/10.1016/j.compositesa.2008.04.001>
15. Dhanawade A, Kumar S (2017) Experimental study of delamination and kerf geometry of carbon epoxy composite machined by abrasive water jet. *Journal of Composite Materials* 51:3373–3390 . <https://doi.org/10.1177/0021998316688950>
16. Ibraheem HMA, Iqbal A, Hashemipour M (2015) Numerical optimization of hole making in GFRP composite using abrasive water jet machining process. *Journal of the Chinese Institute of Engineers* 38:66–76 . <https://doi.org/10.1080/02533839.2014.953240>
17. Alberdi A, Artaza T, Suárez A, Rivero A, Girot F (2016) An experimental study on abrasive waterjet cutting of CFRP/Ti6Al4V stacks for drilling operations. *Int J Adv Manuf Technol* 86:691–704 . <https://doi.org/10.1007/s00170-015-8192-x>
18. Dhakal HN, Ismail SO, Ojo SO, Paggi M, Smith JR (2018) Abrasive water jet drilling of advanced sustainable bio-fibre-reinforced polymer/hybrid composites: a comprehensive analysis of machining-induced damage responses. *Int J Adv Manuf Technol* 99:2833–2847 . <https://doi.org/10.1007/s00170-018-2670-x>
19. Chen L, Lemma E, Siores E, Wang J (2002) Study of Cutting Fiber-reinforced Composites by using Abrasive Water-jet with Cutting Head Oscillation. *Composite Structures* 57: . [https://doi.org/10.1016/S0263-8223\(02\)00097-1](https://doi.org/10.1016/S0263-8223(02)00097-1)
20. Li M, Huang M, Yang X, Li S, Wei K (2018) Experimental study on hole quality and its impact on tensile behavior following pure and abrasive waterjet cutting of plain woven CFRP laminates. *Int J Adv Manuf Technol* 99:2481–2490 . <https://doi.org/10.1007/s00170-018-2589-2>
21. Liu D, Tang Y, Cong WL (2012) A review of mechanical drilling for composite laminates. *Composite Structures* 94:1265–1279 . <https://doi.org/10.1016/j.compstruct.2011.11.024>

22. Vigneshwaran S, Uthayakumar M, Arumugaprabu V (2018) Abrasive water jet machining of fiber-reinforced composite materials. *Journal of Reinforced Plastics and Composites* 37:230–237 .
<https://doi.org/10.1177/0731684417740771>
23. WARDJet Corporation (2019) Waterjet Piercing Techniques and When to Use Them. In: WARDJet.
<https://wardjet.com/news/waterjet-piercing-techniques>. Accessed 22 Apr 2021
24. OMAX Corporation (2016) 4 Piercing Methods In Abrasive Waterjet Machining. In: OMAX.
<https://www.omax.com/news/blog/4-piercing-methods-abrasive-waterjet-machining>. Accessed 22 Apr 2021
25. Fredin J, Jönsson A (2011) Experimentation on Piercing with Abrasive Waterjet. *International Journal of Industrial and Manufacturing Engineering* 59:2393–2399
26. Olsen J.H. (2007) Recent developments in abrasive jet software.
<https://www.thefabricator.com/thefabricator/article/waterjetcutting/recent-developments-in-abrasive-jet-software>. Accessed 22 Apr 2021
27. Rabani A, Marinescu I, Axinte D (2012) Acoustic emission energy transfer rate: A method for monitoring abrasive waterjet milling. *International Journal of Machine Tools and Manufacture* 61:80–89 .
<https://doi.org/10.1016/j.ijmachtools.2012.05.012>
28. Axinte DA, Kong MC (2009) An integrated monitoring method to supervise waterjet machining. *CIRP Annals* 58:303–306 . <https://doi.org/10.1016/j.cirp.2009.03.022>
29. Pahuja R, Ramulu M (2019) Surface quality monitoring in abrasive water jet machining of Ti6Al4V–CFRP stacks through wavelet packet analysis of acoustic emission signals. *Int J Adv Manuf Technol* 104:4091–4104 . <https://doi.org/10.1007/s00170-019-04177-0>

Figures

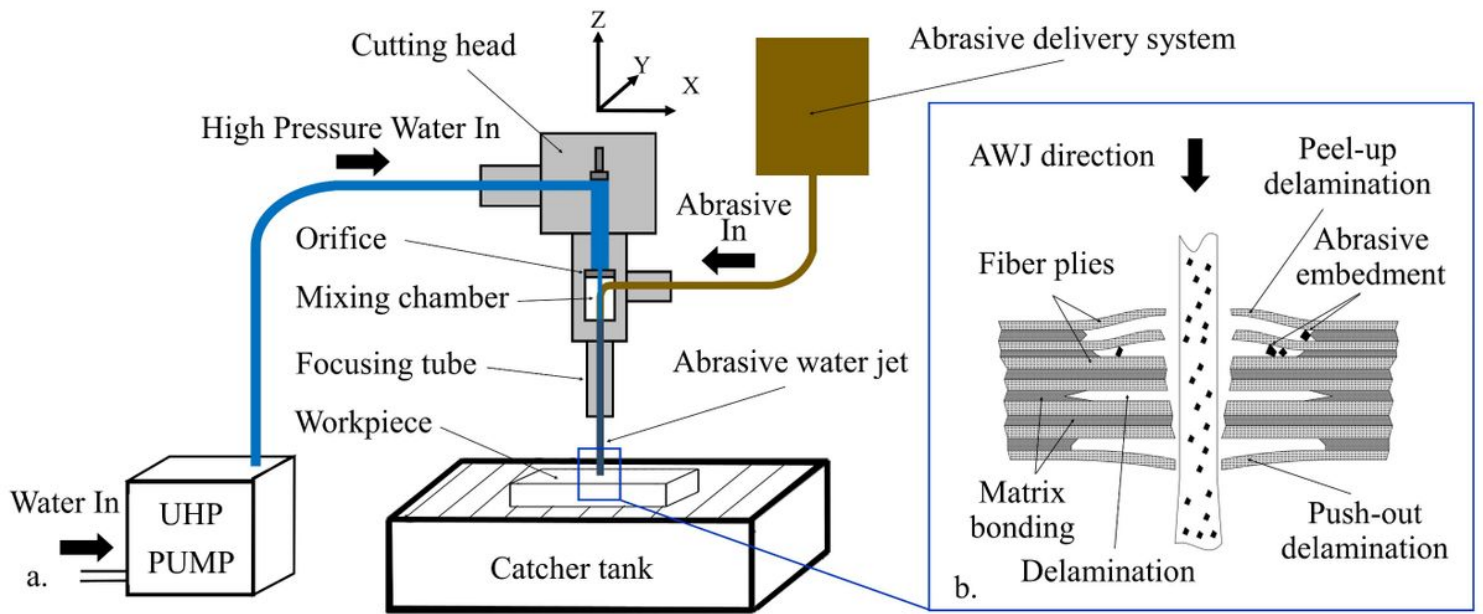


Figure 1

The working principle of composite material piercing through AWJ: a. The AWJ working principle; b. The mechanism of composite material delamination.

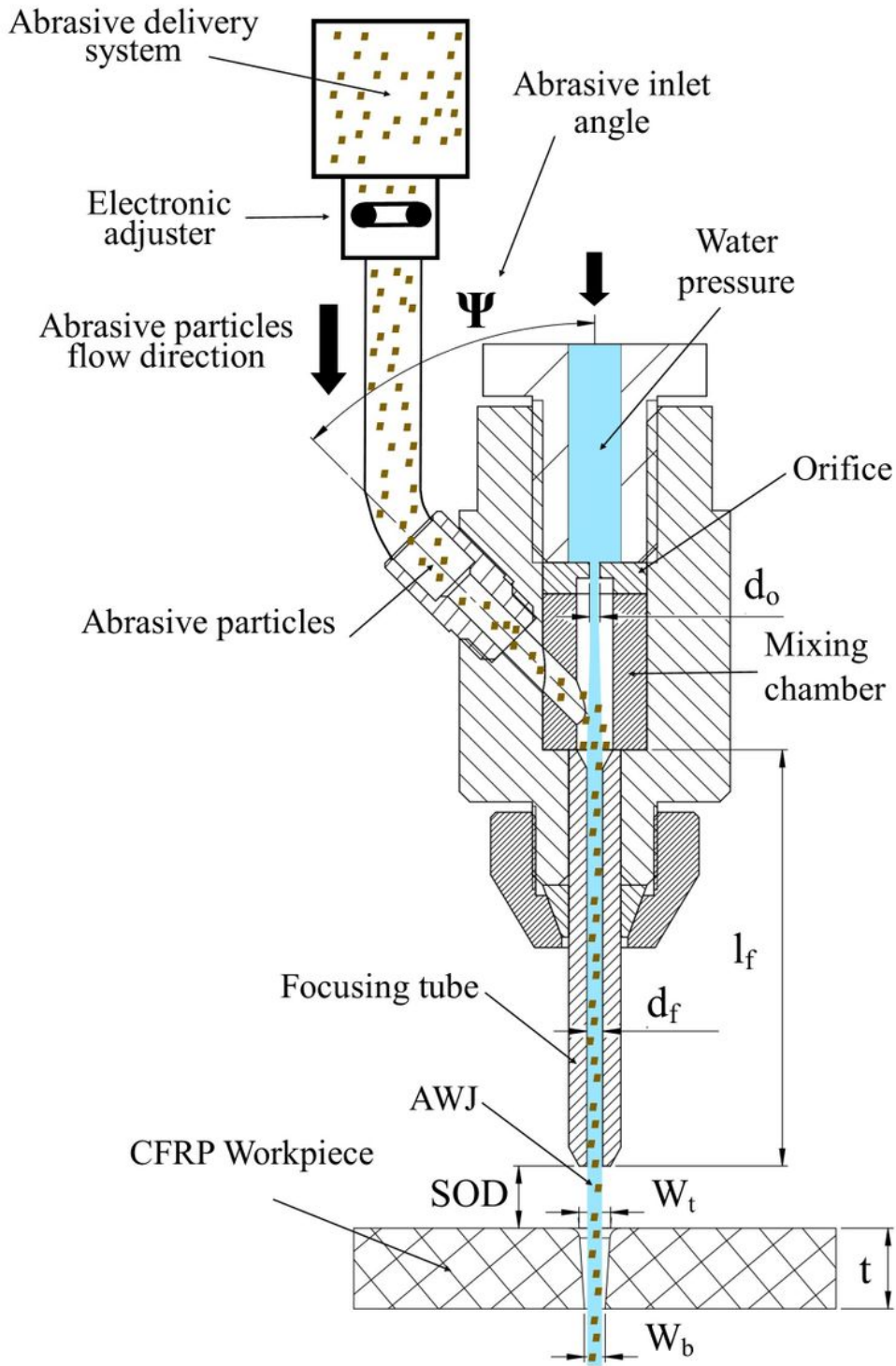


Figure 2

The proposed cutting system

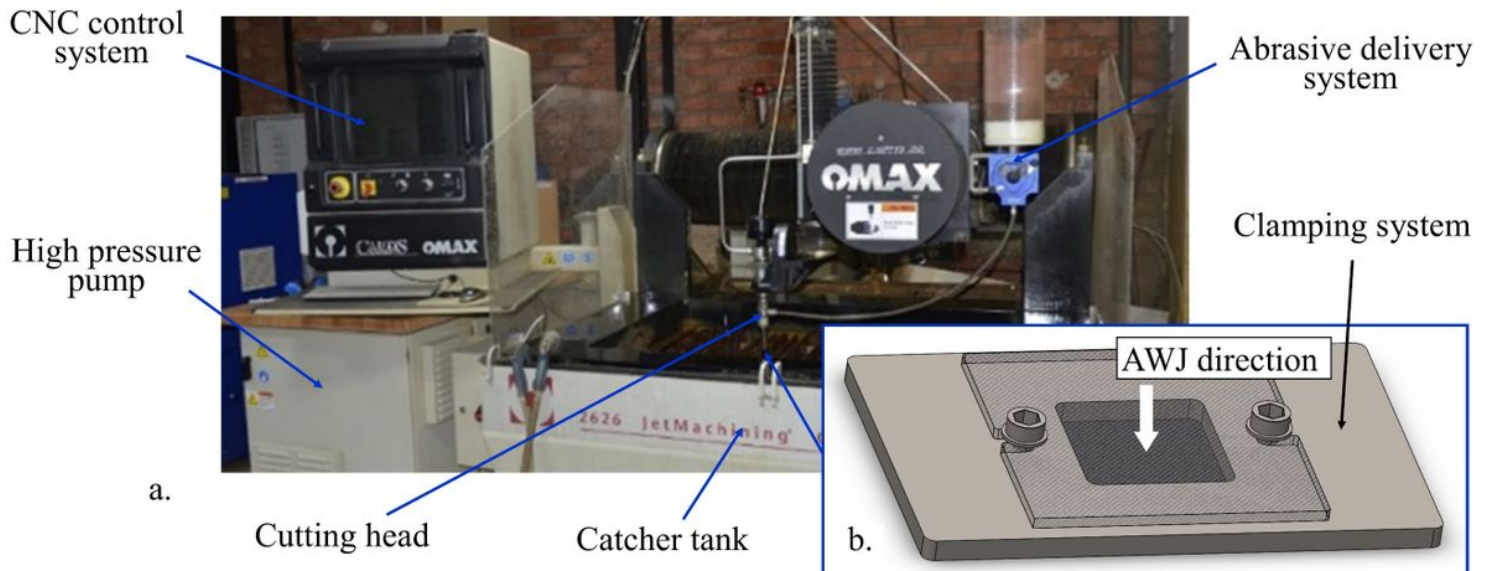


Figure 3

Experimental setup: a. AWJ equipment Omax 2626; b. The clamping system.

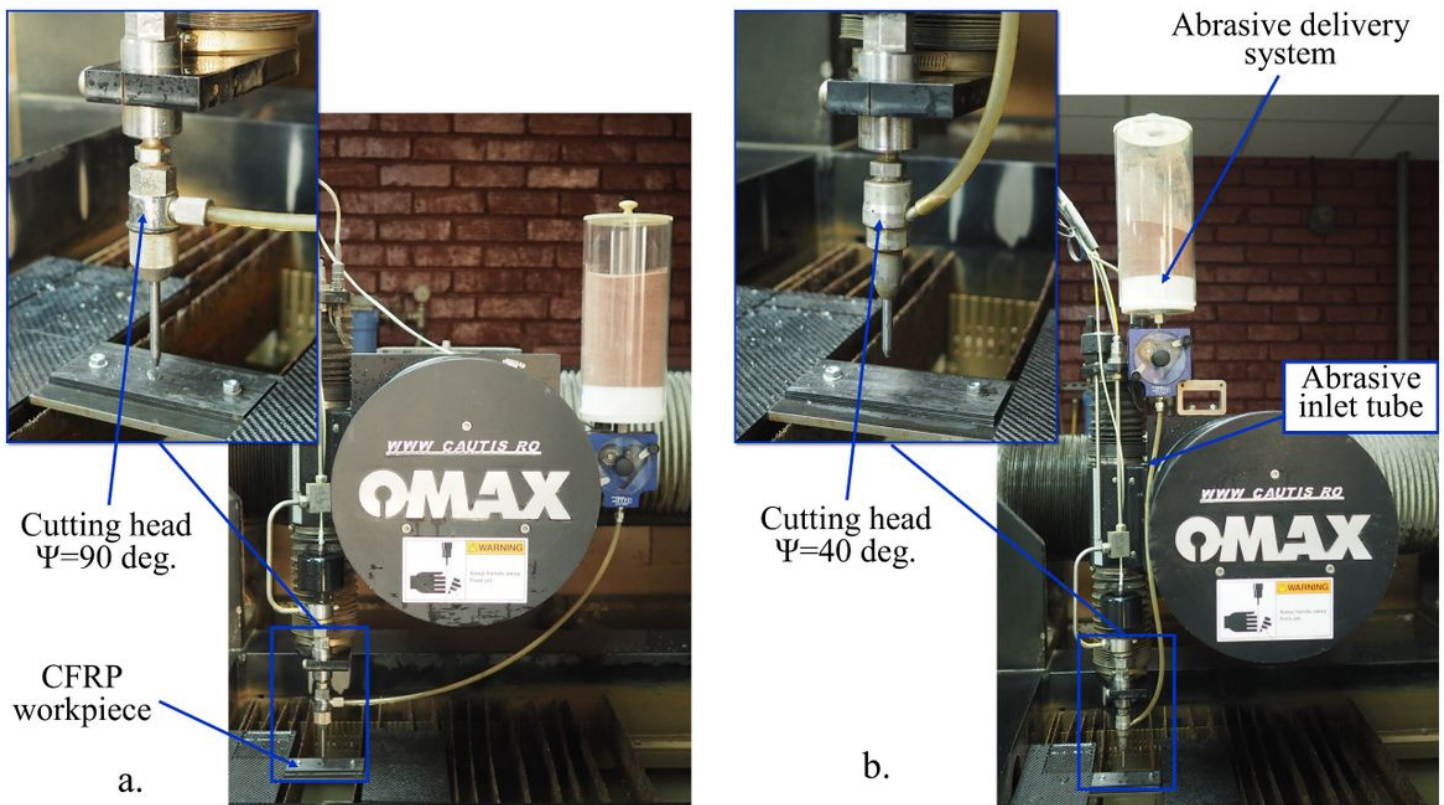


Figure 4

The cutting systems used in the experimental study: a. The conventional cutting system (CS90); b. The proposed cutting system for composite materials piercing (CS40).

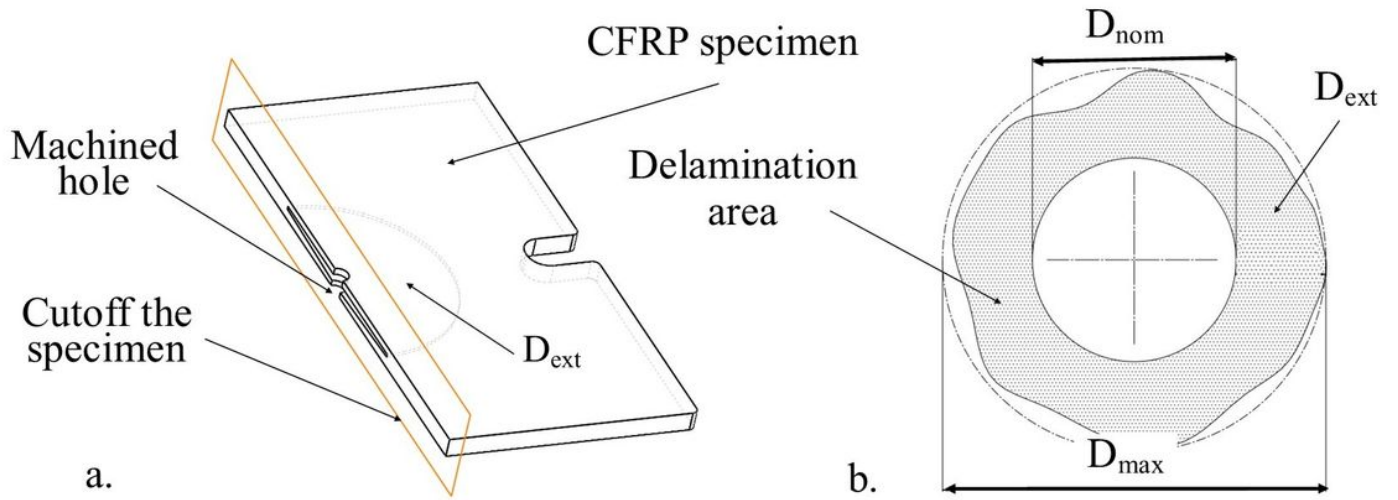


Figure 5

Experimental results evaluation: a. The position to cutoff the specimens, b. The delamination area evaluation.

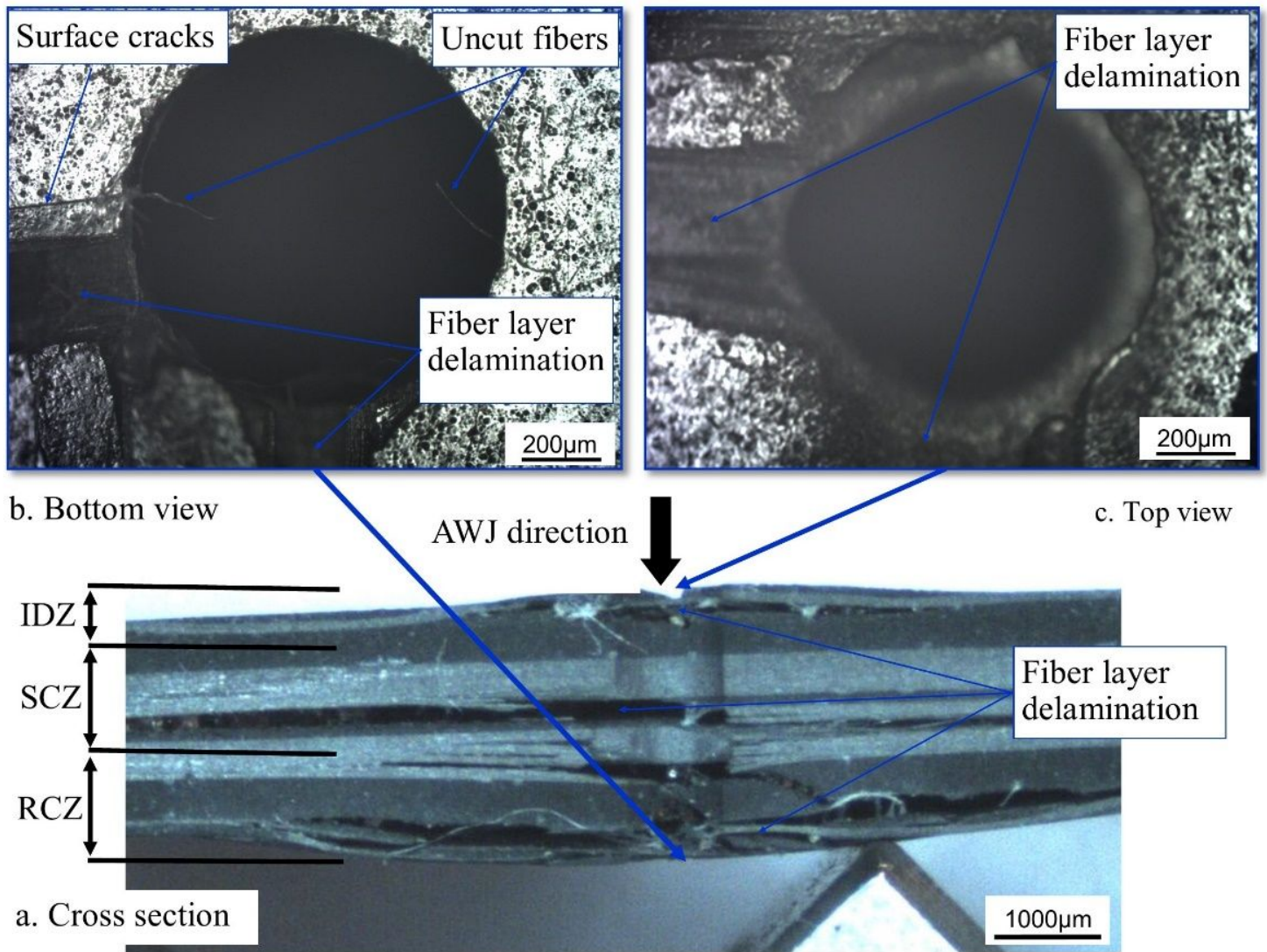


Figure 6

Delamination (Dext = 48.2 mm) observed in experimental run no. 8 made with CS90, ($P = 350 \text{ MPa}$, $SOD = 3.5 \text{ mm}$, $ma = 0.45 \text{ kg/min}$).

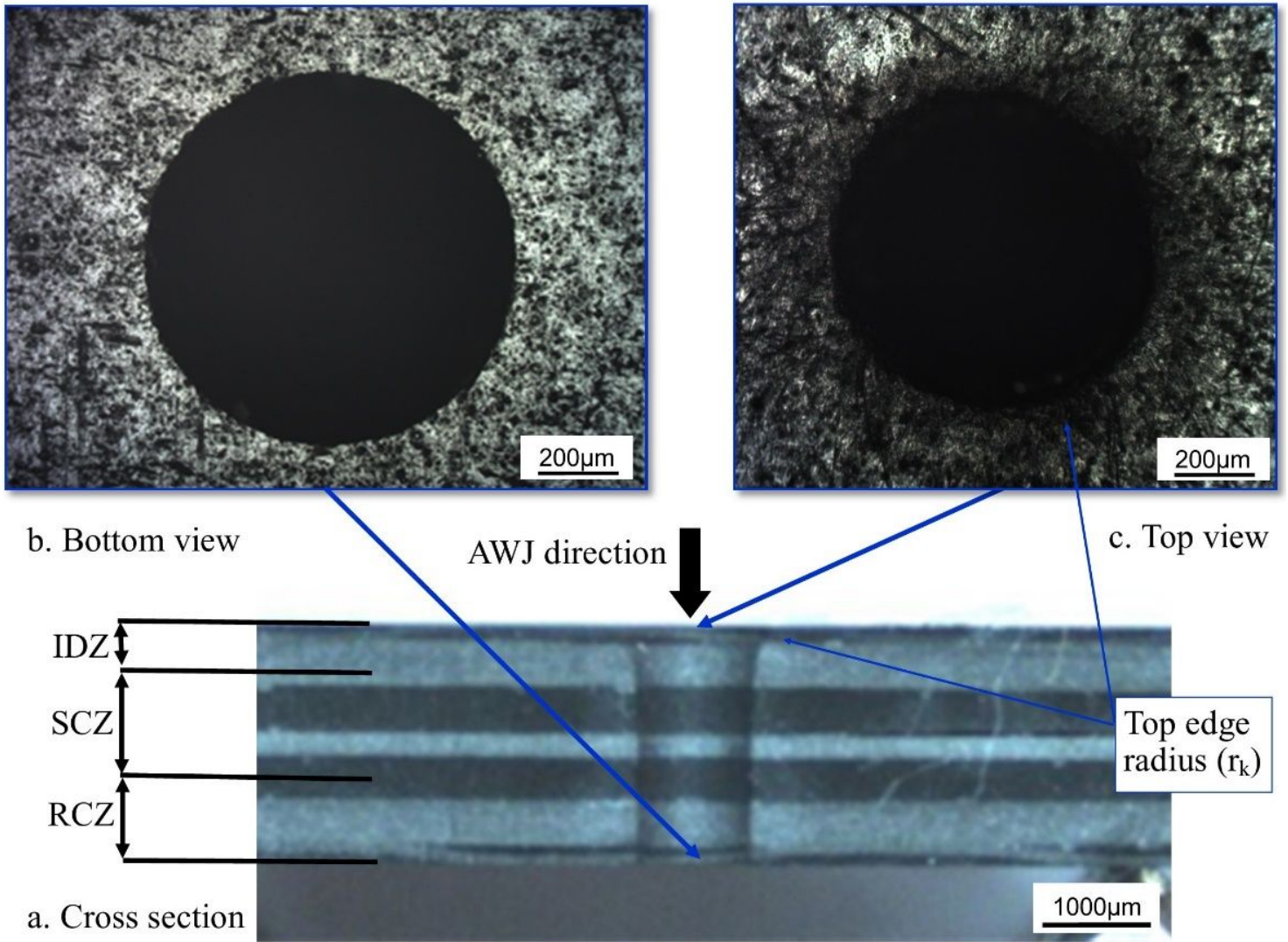


Figure 7

Hole obtained without delamination in experimental run no. 12, made with the CS40, ($P = 100$ MPa, $SOD = 3.5$ mm, $ma = 0.45$ kg/min).

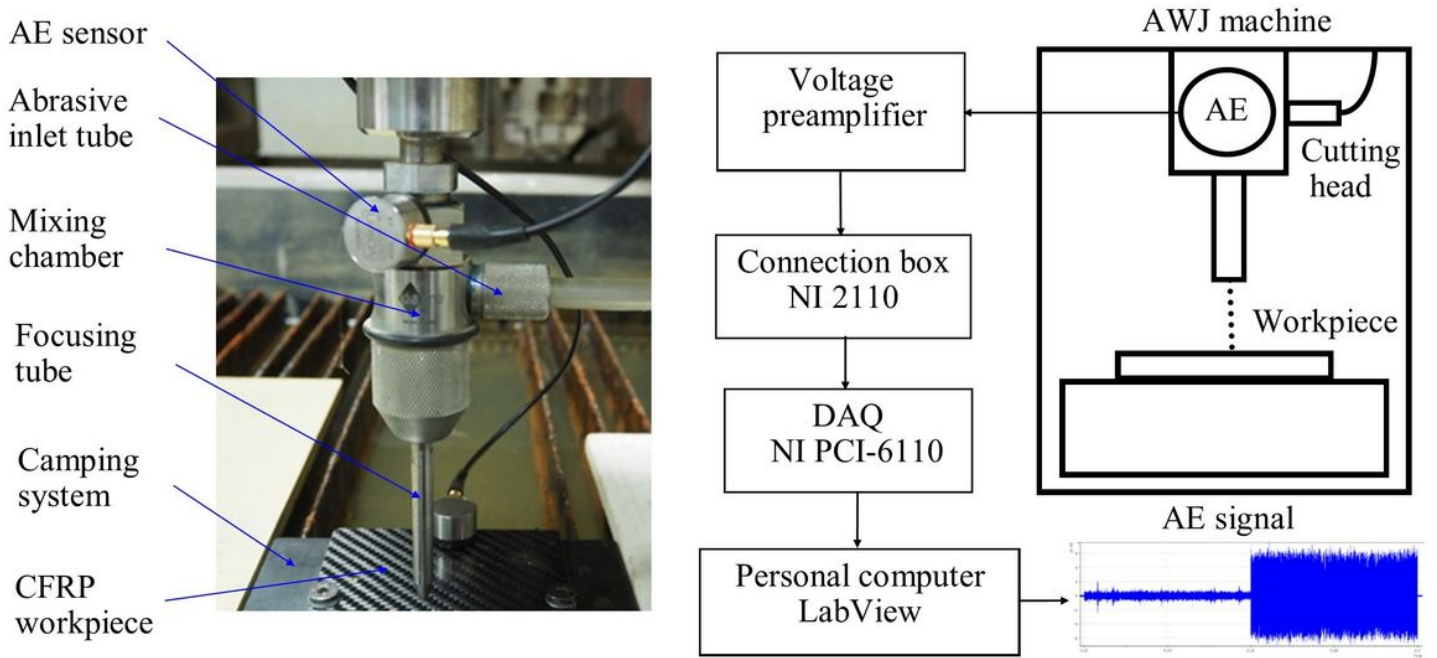


Figure 8

The experimental setup for AWJ piercing monitoring via AE.

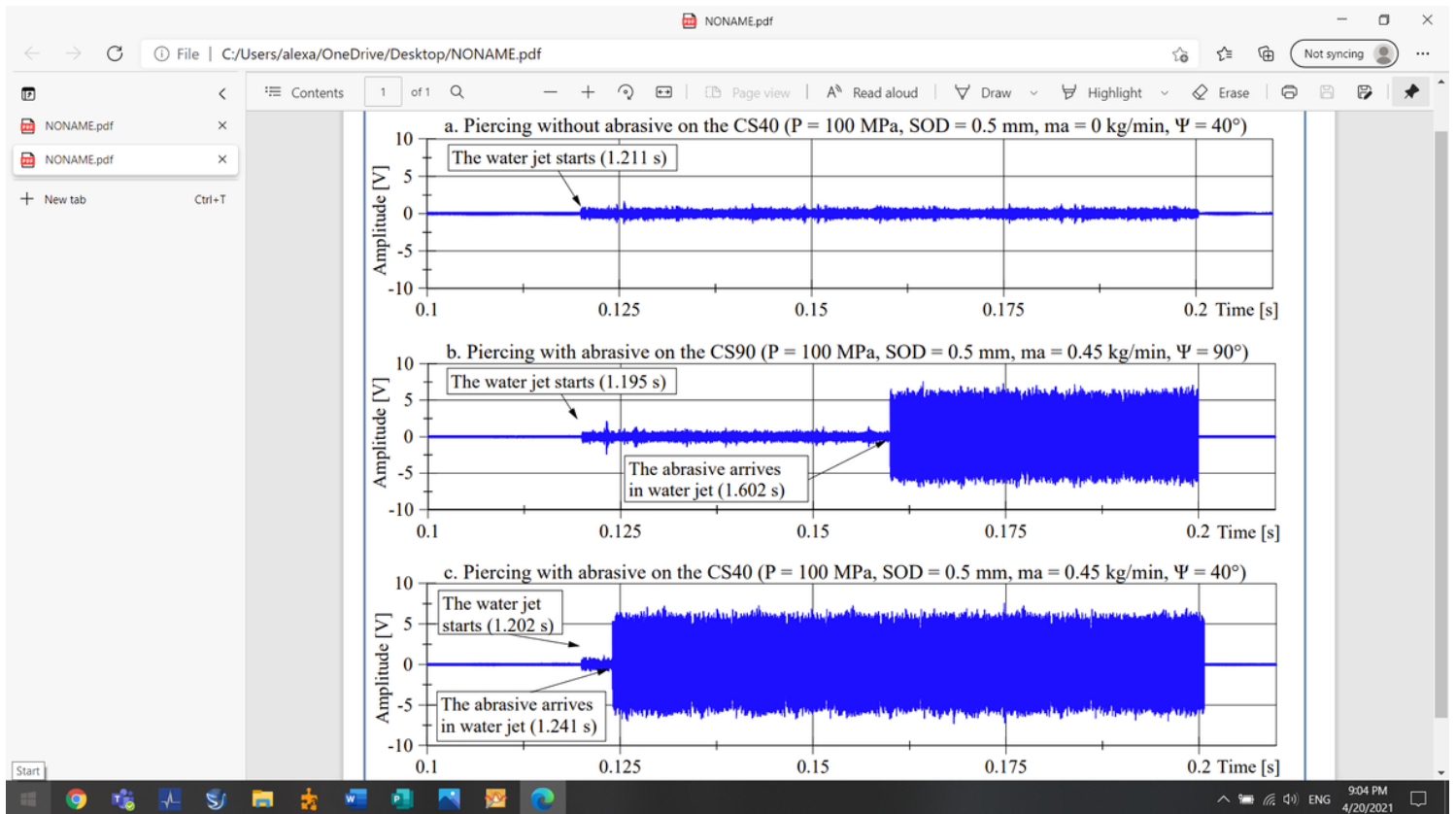


Figure 9

Acoustic emission signals in the time domain for the three cases: a. WJ piercing without abrasive; b. AWJ piercing using the CS90; c. AWJ piercing using the CS40.

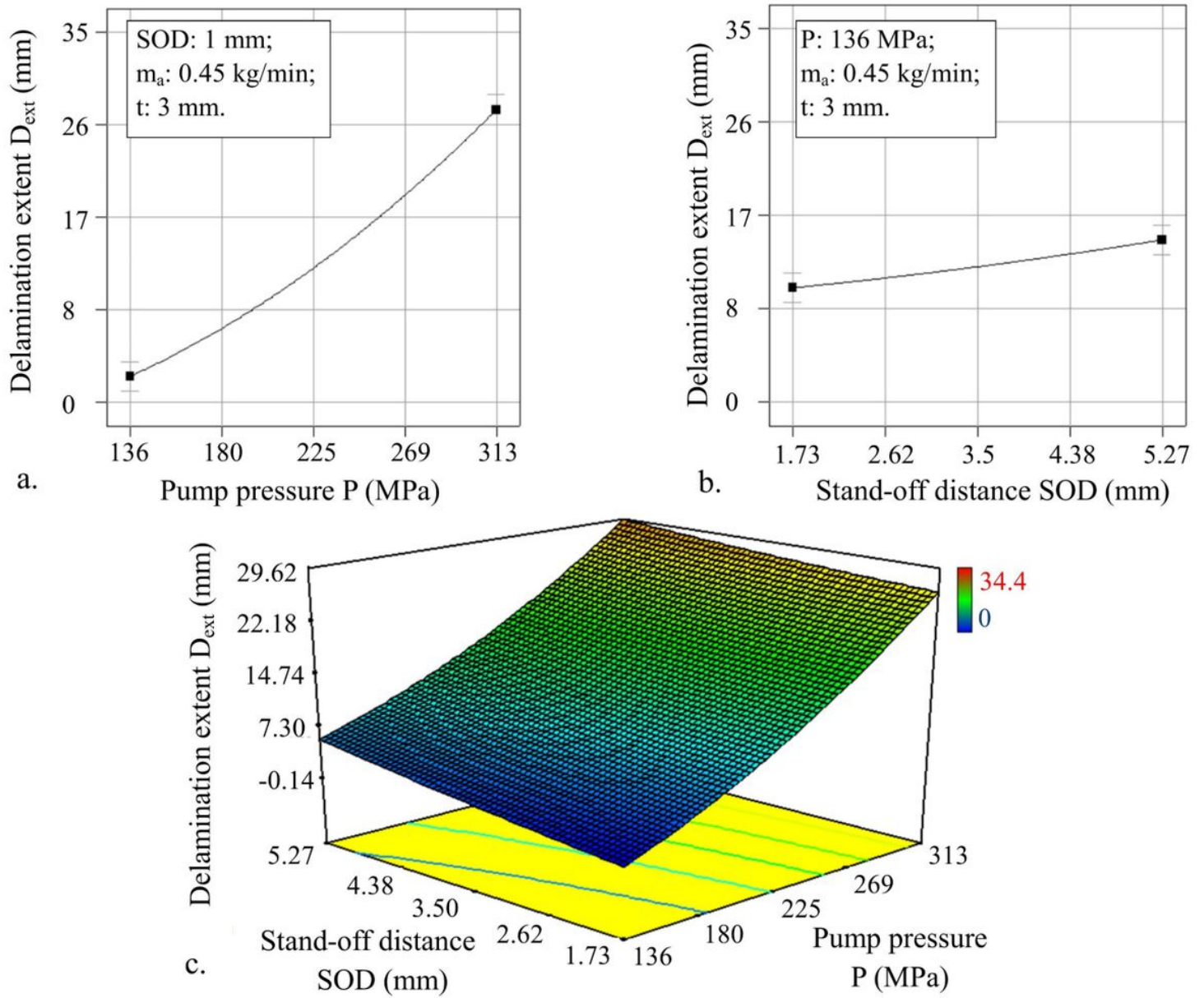


Figure 10

Graphical representation of the response surface model for the delamination extent: (a) Effect of P on D_{ext} ; (b) Effect of SOD on D_{ext} ; (c) The 3D surface of the response surface model.